

# Carotid Plaque Phenotyping by Correlating Plaque Morphology from Computed Tomography Angiography with Transcriptional Profiling

Eva Karlöf<sup>a,b</sup>, Andrew Buckler<sup>b,c</sup>, Moritz L. Liljeqvist<sup>b</sup>, Mariette Lengquist<sup>b</sup>, Malin Kronqvist<sup>b</sup>, Mawaddah A. Toonsi<sup>b</sup>, Lars Maegdefessel<sup>d,e</sup>, Ljubica P. Matic<sup>b</sup>, Ulf Hedin<sup>a,b,\*</sup>

<sup>a</sup> Department of Vascular Surgery, Karolinska University Hospital, Stockholm, Sweden

<sup>b</sup> Department of Molecular Medicine and Surgery, Karolinska Institutet, Stockholm, Sweden

<sup>c</sup> Elucid Bioimaging, Boston, MA, USA

<sup>d</sup> Department of Medicine, Karolinska Institutet, Stockholm, Sweden

<sup>e</sup> Department of Vascular and Endovascular Surgery, Klinikum rechts der Isar, Technical University Munich, Munich, Germany

## WHAT THIS PAPER ADDS

Using analytical software for processing of pre-operative carotid computed tomography angiography images and transcriptomic analysis of corresponding carotid endarterectomy specimens, plaque morphological features were demonstrated to reflect prevalent biological processes relevant for plaque stability and instability. Plaque morphology was also superior to measurement of the degree of stenosis in prediction of symptomatology, which supports implementation of imaging of plaque morphology for improved risk stratification and management of patients with carotid stenosis.

**Objective:** Ischaemic strokes can be caused by unstable carotid atherosclerosis, but methods for identification of high risk lesions are lacking. Carotid plaque morphology imaging using software for visualisation of plaque components in computed tomography angiography (CTA) may improve assessment of plaque phenotype and stroke risk, but it is unknown if such analyses also reflect the biological processes related to lesion stability. Here, we investigated how carotid plaque morphology by image analysis of CTA is associated with biological processes assessed by transcriptomic analyses of corresponding carotid endarterectomies (CEAs).

**Methods:** Carotid plaque morphology was assessed in patients undergoing CEA for symptomatic or asymptomatic carotid stenosis consecutively enrolled between 2006 and 2015. Computer based analyses of pre-operative CTA was performed to define calcification, lipid rich necrotic core (LRNC), intraplaque haemorrhage (IPH), matrix (MATX), and plaque burden. Plaque morphology was correlated with molecular profiles obtained from microarrays of corresponding CEAs and models were built to assess the ability of plaque morphology to predict symptomatology.

**Results:** Carotid plaques ( $n = 93$ ) from symptomatic patients ( $n = 61$ ) had significantly higher plaque burden and LRNC compared with plaques from asymptomatic patients ( $n = 32$ ). Lesions selected from the transcriptomic cohort ( $n = 40$ ) with high LRNC, IPH, MATX, or plaque burden were characterised by molecular signatures coupled with inflammation and extracellular matrix degradation, typically linked with instability. In contrast, highly calcified plaques had a molecular signature signifying stability with enrichment of profibrotic pathways and repressed inflammation. In a cross validated prediction model for symptoms, plaque morphology by CTA alone was superior to the degree of stenosis.

**Conclusion:** The study demonstrates that CTA image analysis for evaluation of carotid plaque morphology, also reflects prevalent biological processes relevant for assessment of plaque phenotype. The results support the use of CTA image analysis of plaque morphology for risk stratification and management of patients with carotid stenosis.

**Keywords:** Atherosclerotic plaque, Carotid stenosis, Computer tomography angiography, Gene expression

Article history: Received 5 January 2021, Accepted 11 July 2021, Available online 10 September 2021

© 2021 The Author(s). Published by Elsevier B.V. on behalf of European Society for Vascular Surgery. This is an open access article under the CC BY license (<http://creativecommons.org/licenses/by/4.0/>).

\* Corresponding author. Division of Vascular Surgery, Department of Molecular Medicine and Surgery, Bioclinicum J8:20, Karolinska University Hospital and Karolinska Institutet, 171 64, Stockholm, Sweden.

E-mail address: [ulf.hedin@ki.se](mailto:ulf.hedin@ki.se) (Ulf Hedin).

 @ki\_vasc

1078-5884/© 2021 The Author(s). Published by Elsevier B.V. on behalf of European Society for Vascular Surgery. This is an open access article under the CC BY license (<http://creativecommons.org/licenses/by/4.0/>).

<https://doi.org/10.1016/j.ejvs.2021.07.011>

## INTRODUCTION

Unstable atherosclerotic plaques in the carotid bifurcation contribute to ischaemic strokes but methods to identify lesions at high risk are lacking.<sup>1</sup> Risk stratification of patients with carotid stenosis is currently based on

measurements of stenosis and stroke preventive treatment, carotid endarterectomy (CEA), restricted to patients with high degree stenosis,<sup>2</sup> resulting in moderate procedural efficacy.<sup>3</sup> Non-invasive imaging to characterise carotid plaque morphology holds promise for improved risk prediction based on plaque biology, rather than the degree of stenosis,<sup>1,4</sup> and the recent European Society for Vascular Surgery guidelines advocate the assessment of additional plaque parameters in high risk asymptomatic patients.<sup>2</sup> Establishing an association between plaque morphology and biological processes relevant for plaque instability would support implementation of carotid plaque imaging for improved patient management.

Unstable atherosclerotic plaques are characterised by inflammation, accumulation of a large lipid rich necrotic core (LRNC), intraplaque neovascularisation and bleeding (intraplaque haemorrhage; IPH), a thin fibrous cap from extracellular matrix degradation and depletion of smooth muscle cells (SMCs), and generally less calcification (CALC) than stable, asymptomatic lesions.<sup>5</sup> Non-invasive imaging such as ultrasound, computed tomography angiography (CTA) and magnetic resonance imaging (MRI) may distinguish morphological features associated with unstable carotid lesions.<sup>6</sup> Although most of these imaging modalities have limitations, CTA offers practical advantages and can distinguish plaque tissue based on Hounsfield units (HU) but suffers from artefacts from calcium blooming, low soft tissue contrast, and overlapping material densities of LRNC and IPH.<sup>7</sup> However, these limitations can be mitigated with CTA post-processing using analytical software that improves characterisation of plaque morphology.<sup>8–13</sup>

Combining carotid CTA with molecular analyses of plaque tissue permits the association of imaging biomarkers with pathophysiological processes. We recently demonstrated that carotid plaque macrocalcification, quantified in CTA, correlated with biological processes associated with a stable plaque phenotype. As assessed by transcriptomic analyses, highly calcified lesions were enriched in biological pathways associated with SMCs and fibrosis whereas pathways typically associated with instability were repressed.<sup>14</sup> Here, the objective was to develop this approach further using computer based CTA image analysis for determination of plaque morphology, followed by correlations with symptomatology and molecular signatures from corresponding CEAs.

## MATERIALS AND METHODS

### *Patient cohorts*

Patients undergoing surgery for high grade (> 50% North American Symptomatic Carotid Endarterectomy Trial [NASCET])<sup>3</sup> carotid stenosis, assessed by pre-operative carotid CTA, were enrolled consecutively in the study between 2006 and 2015. Qualifying symptoms in patients with carotid stenosis were determined by a neurologist and defined as transient ischaemic attack (TIA), minor stroke and *amaurosis fugax* (retinal TIA), and surgery performed

within two weeks after the event. Patients without qualifying symptoms within three months prior to surgery were categorised as asymptomatic, and patients with atrial fibrillation were excluded. For gene expression analyses (transcriptomic cohort), CEA specimens were collected at surgery and retained within the Biobank of Karolinska Endarterectomies. Plaques were divided transversely at the most stenotic part; the proximal half of the lesion used for RNA preparation while the distal half was processed for histology as described previously.<sup>14,15</sup>

### *Computed tomography angiography and image analysis*

Carotid CTA was performed pre-operatively as described previously.<sup>14</sup> Reconstructed images (0.625 mm) were analysed in a blinded fashion by one observer (E.K) using the *vascuCAP*® (Elucid Bioimaging Inc., Boston, MA) software.<sup>8–13</sup> The software creates 3D segmentations with improved resolution and soft tissue plaque component differentiation. A patient specific 3D point spread function restores image intensities and enables discrimination of tissue types such as LRNC and IPH. To avoid limitations of fixed thresholds, accuracy is achieved by algorithms that account for distributions of tissue constituents rather than assuming constant material density ranges. Here, the software interprets the HU of adjacent voxels by maximising criteria that mimic expert annotated histology, mitigating variation between scanners, reconstruction kernels, and contrast levels.

The external carotid artery was excluded from analyses and the lumen and wall of the common and internal carotid artery evaluated automatically and, when needed, edited manually. Thereafter, the whole lesion was processed for analysis except in the transcriptomics cohort, where only the proximal half of the lesion was analysed, corresponding to the tissue used for microarray analysis.

The plaque was defined by tissue components: LRNC; CALC; IPH; and MATX (representing plaque tissue not detected as either LRNC, CALC, or IPH), with the proportion of the total wall volume (VolProp) quantified. Structural features included: plaque burden (proportion of total vessel volume or area), minimal fibrous cap thickness (shortest distance from edge of LRNC to lumen in  $\mu\text{m}$ ) and stenosis degree (NASCET).<sup>3</sup>

### *Gene expression analyses*

Gene expression was analysed by microarrays as described previously.<sup>14,15</sup> In brief, RNA was extracted from CEAs in the transcriptomics cohort ( $n = 40$ ) and gene expression analysed in Affymetrix HTA 2.0 arrays in one batch (Affymetrix, Santa Clara, CA). Annotation was based on the Hg19 genome build, NCBI genome version GRCh37, and NetAffx build 34, for all 70 523 probesets. Signal space transformation and robust multiarray average normalisation was performed on the Transcriptome Analysis Console software (Thermo Fisher Scientific) and processed gene expression

data returned in log2 scale. The microarray dataset is available from Gene Expression Omnibus (GSE125771).

### Histochemistry

CEA specimens were fixed in 4% formaldehyde and calcified plaques decalcified in Modified Decalcification Solution (HL24150.1000). Specimens were rinsed, dehydrated, embedded in paraffin and axially sectioned at selected distances from the bifurcation and the origin of the external carotid as guided by CTA and the location of defined plaque components in processed images. Sections were deparaffinised with Histolab clear (Histolab, Sweden) and rehydrated. Calcification was visualised with Alizarin Red (Sigma-Aldrich, Germany), followed by dehydration in acetone and acetone-xylene (1:1). IPH was detected by Perl's Blue staining (Histolab, Sweden), rinsed with water, and counterstained in nuclear fast red. Intraplaque lipids were detected with Oil Red O (Sigma O1391), slides rinsed in 60% isopropanol, and counterstained with HTX (Mayers, Sigma-Aldrich, Germany). All staining was performed according to the manufacturer's instructions.

### Bio-informatic and statistical analysis

Analyses of differential gene expression was performed in patients selected from the transcriptomics cohort using the volume proportions of components and structural

categories where gene expression profiles of plaques with the highest measured values were compared with those with the lowest in order to optimise identification of biological processes associated with either of the categories and to mitigate the inherent heterogeneity in carotid plaque morphology (10 vs. 10 for components and 5 vs. 5 for structural category). In the IPH subgroup, the lowest values were all in highly calcified plaques, which is why 5 vs. 5 were only selected from low calcified plaques to avoid confounding (Table 1). The groups were analysed using limma<sup>16</sup> with empirical Bayes moderation of the standard errors towards a global value, implemented in Transcriptome Analysis Console (Thermo Fisher Scientific).

Significantly differentially expressed genes and ontologies were identified with false discovery rate (FDR)  $q < .05$  and differentially expressed genes displayed in volcano plots. For the identification of biological pathways, ranked lists of genes according to  $p$  value were processed through gene set enrichment analysis<sup>17</sup> (v. 4.1.0; GO Biological Processes c5.go.bp.v7.2.symbols.gmt) and then run through Cytoscape (v.3.8.2) with Java (v.11.0.6) where the cut off  $p$  value and FDR  $q$  value were both set to  $< .005$  in order to visualise top (upregulated) and bottom (downregulated) ontologies and pathways. Clusters were created with the AutoAnnotate function as described previously.<sup>18</sup>

Correlations between different types of plaque morphology (components and structure) were performed in

**Table 1.** Demographics of patients with carotid artery stenosis describing the whole cohort, patients with carotid endarterectomy specimens analysed by microarrays (transcriptomics cohort), and the sub-cohorts created using the volume proportions (%) of the components lipid rich necrotic core (LRNC), calcification (CALC), intraplaque haemorrhage (IPH), matrix (MATX), and the structural categories plaque burden and the maximum degree of stenosis (Max stenosis), where plaques with the highest measured values (high) were compared with those with the lowest measured values (low)

Patient characteristics	Whole cohort (n=93)	Transcript-omics cohort (n=40)	LRNC		CALC		IPH		MATX		Plaque burden		Max stenosis	
			High 8–27% (n=10)	Low 0–1% (n=10)	High 30–52% (n=10)	Low 0–3% (n=10)	High 4.9–7.3% (n=5)	Low 0–0.2% (n=5)	High 83–91% (n=10)	Low 44–62% (n=10)	High 65–74% (n=5)	Low 47–54% (n=5)	High 94–99% (n=5)	Low 7–47% (n=5)
Mean age – y	70.8	71.2	73.1	69.3	71.6	68.8	73.1	69.3	71.3	71.2	73.7*	64.6*	68.4	73.2
Male sex	68 (73)	29 (72)	4 (40)	2 (20)	6 (40)	7 (70)	2 (40)	2 (40)	8 (80)	7 (70)	2 (40)	4 (80)	5 (100)	4 (80)
Mean BMI – kg/m <sup>2</sup>	26.63	26.24	26.11	26.83	24.56	26.9	28.76	25.71	27.81	25.03	26.94	26.23	25.47	27.71
Smoking	17 (18)	7 (18)	2 (20)	2 (20)	3 (30)	2 (20)	1 (20)	1 (20)	1 (10)	2 (20)	3 (60)	1 (20)	1 (20)	0 (0)
<b>Comorbidities</b>														
Previous MI	15 (16)	4 (10)	2 (20)	0 (0)	0 (0)	2 (20)	0 (0)	1 (20)	0 (0)	0 (0)	1 (20)	0 (0)	1 (20)	0 (0)
Angina pectoris	18 (19)	8 (20)	2 (20)	3 (30)	3 (30)	2 (20)	0 (0)	0 (0)	1 (10)	2 (20)	1 (20)	1 (20)	2 (40)	1 (20)
Diabetes	22 (24)	9 (23)	1 (10)	3 (30)	3 (30)	2 (20)	0 (0)	1 (20)	3 (30)	3 (30)	0 (0)	1 (20)	1 (20)	1 (20)
<b>Medication</b>														
Lipid lowering	88 (95)	38 (95)	10 (100)	10 (100)	9 (90)	10 (100)	5 (100)	4 (80)	10 (100)	10 (100)	4 (80)	5 (100)	4 (80)	5 (100)
Anti-hypertensives	69 (74)	32 (80)	8 (80)	10 (100)	9 (90)	8 (80)	4 (80)	4 (80)	8 (80)	10 (100)	3 (60)	4 (80)	4 (80)	4 (80)
Symptomatic	61 (66)	20 (50)	6 (60)	6 (60)	6 (60)	4 (40)	2 (40)	3 (60)	5 (50)	5 (50)	3 (60)	1 (20)	3 (60)	2 (40)
Asymptomatic	32 (34)	20 (50)	4 (40)	4 (40)	4 (40)	6 (60)	3 (60)	2 (40)	5 (50)	5 (50)	2 (40)	4 (80)	2 (40)	3 (60)

Data are presented as  $n$  (%) unless stated otherwise. Group analysis performed with two sided Student's  $t$  test and Fisher's exact test. BMI = body mass index; MI = myocardial infarction.

\*  $p = .031$ .

the whole cohort, with univariable analysis using GraphPad Prism 8 correlation matrix and Pearson's coefficient, and correlogram created in R (package *corrplot2017*, v 0.84). Associations between symptomatology and plaque morphology were explored with Spearman's coefficient and two sided Student's *t* test assuming normal distribution and equal standard deviation. Variables not fulfilling the criteria for normal distribution (MinCapThickness) were log transformed into normality before the *t* test.

### Prediction modelling

Single variable analysis was performed to explore the relationships between individual measurements. Predictive modelling comprised the development of multivariable models using four predictor sets: plaque morphology predictors alone (e.g., LRNCVolProp, MATXVol, IPHVol); clinical predictors alone (triglycerides, cholesterol fibrinogen, white blood count, low density lipoprotein, smoking, diabetes, body mass index); a combination of plaque morphology, clinical and demographic (age, sex) predictors; and degree of stenosis (NASCET)<sup>3</sup> category as a baseline. Models were developed with three levels of variation: (1) differing sets of morphology according to physiological rationale; (2) automated optimisation using 10 fold cross validation while simultaneously varying tuning parameter values; and (3) data partitioned such that a training set ( $n = 63$ ) on which the cross validation was performed and a sequestered validation data set to test performance ( $n = 30$ ) were created. Models were optimised using area under the receiver operating characteristic curve (AUROC) and Cohen's Kappa, the former to represent classification effectiveness and the latter to ensure effective class (symptomatic and asymptomatic) prediction to account for class imbalance. Here, the best performing model was built using an averaged neural network (avNNet).<sup>19</sup>

## RESULTS

Ninety-eight patients were enrolled in the study. Of these, five were excluded due to poor CTA image quality, 40 patients were analysed with CTA and CEA transcription profiling (transcriptomics cohort)<sup>14</sup> and 53 patients only with CTA, rendering a total study cohort of  $n = 93$  (Table 1). Comparison between CTA image analysis and histological analysis of corresponding CEA specimens showed concordance between plaque morphology and histology, confirming previous validation of the software,<sup>8,10,11</sup> with accurate visualisation of plaque components obtained from software analysed CTA images (Fig. 1).

### Correlations between plaque morphology and gene expression profiles

To investigate whether carotid plaque features by CTA represented relevant biological processes, plaque morphology was correlated with gene expression obtained

from global genome microarrays. Patients were selected from the transcriptomic cohort with respect to symptomatology in order to reduce confounding, and lesions were ranked by the measured volume proportions of plaque components (LRNC, CALC, IPH, and MATX) or structural categories (Table 1) and compared with corresponding gene expression profiles.

Several of the differentially expressed most upregulated genes in plaques with a large LRNC were related to inflammation such as complement activation, T cells, macrophages, and pro-inflammatory mediators (Fig 2A). In high LRNC lesions, gene set enrichment analysis also showed significant enrichment of biological processes associated with inflammation, accompanied by pathways associated with cholesterol metabolism, extracellular matrix (ECM) disassembly, and bone resorption (Fig. 3A). Among downregulated genes in plaques with a large proportion of LRNC were those related to cell proliferation and endothelial cells and downregulated pathways were dominated by processes related to cell proliferation and calcification (Figs 2A and 3A; Supplementary Table S1A, B).

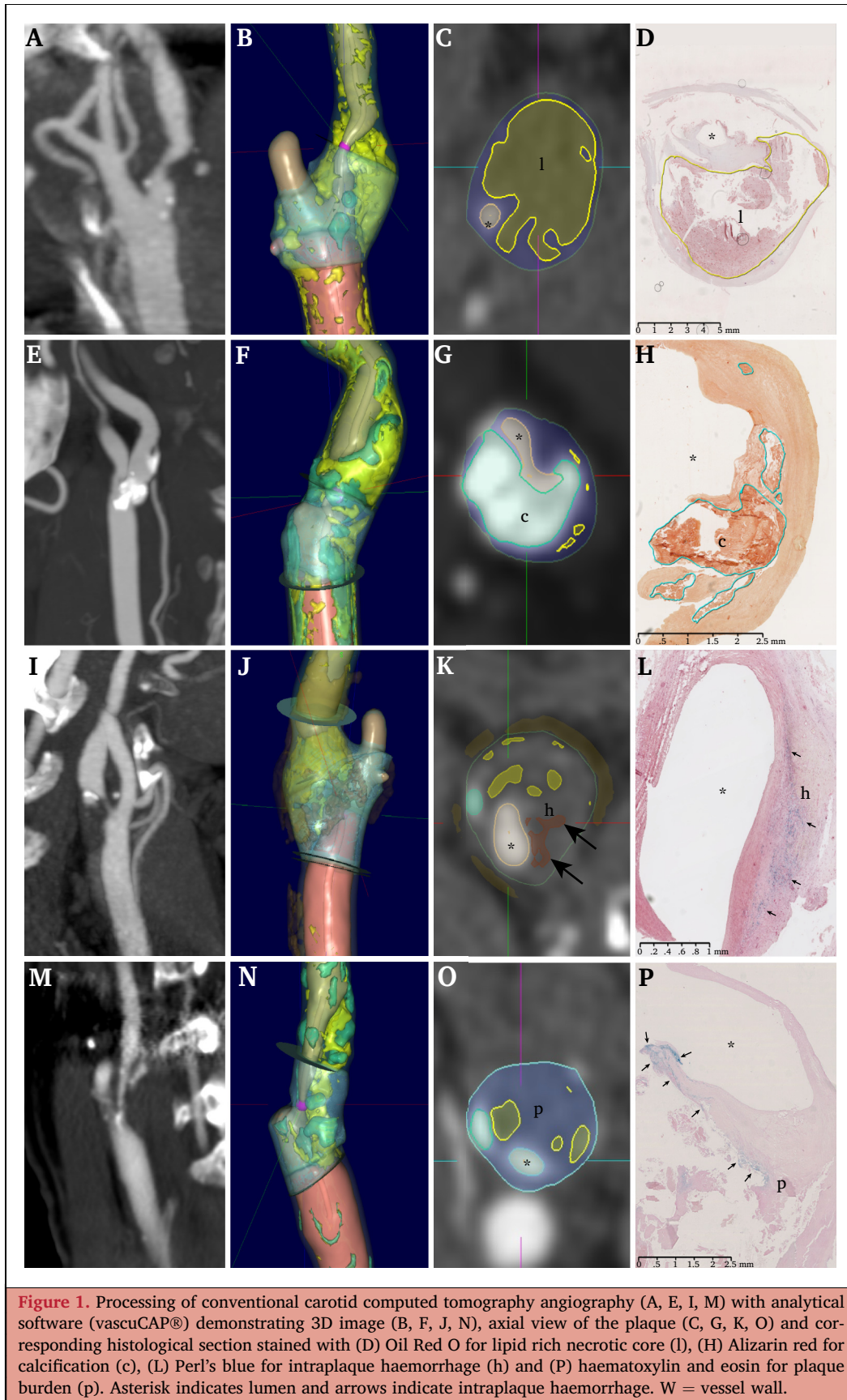
In plaques with a large proportion of CALC, upregulated genes were related to calcification and SMCs (Fig. 2B). The most significantly enriched processes were also associated with SMC function accompanied by enrichment of cell matrix adhesion and ossification (Fig. 3B). Among the repressed genes were those related to ECM degradation, lipid metabolism and inflammation (Fig. 2B). Among downregulated pathways, inflammatory processes were predominant accompanied by ECM and collagen degradation (Figs 2B and 3B; Supplementary Table S2A, B).

In plaques with large IPH, upregulated genes were related to immunoglobulins, platelets, endothelial cells and inflammation (Fig. 2C). Significantly upregulated pathways were related to inflammation and angiogenesis, whereas ECM organisation, SMC migration and contraction were repressed (Fig. 3C; Supplementary Table S3A, B).

Plaques dominated by MATX had upregulated genes associated with lipid metabolism and inflammation. Significantly enriched ontologies were represented by inflammatory processes. In contrast to LRNC rich plaques, enrichment of processes related to ECM degradation was not observed. Repressed genes largely overlapped with those upregulated in plaques with high CALC and downregulated processes were related to SMCs, ECM assembly and ossification (Supplementary Table S4A, B).

Plaques with the largest plaque burden showed upregulation of genes representing lipid metabolism, inflammatory cells, metalloproteinases, and haemoglobin metabolism (Fig. 2D). Enriched pathways were related to inflammation (Fig. 3D). Repressed genes consisted of SMC related ones (Fig. 2D) and downregulated processes were related to SMCs and ossification (Fig. 3D; Supplementary Table S5A, B).

In contrast, analysis of gene expression patterns in plaques with a high vs. low degree of stenosis (NASCET) did not



discriminate any clear patterns by gene set enrichment analysis, and inflammatory pathways were both enriched and repressed (Supplementary Table S6A, B).

### Correlations between plaque features

The observed relationships between plaque components and/or structures are summarised in a correlogram (Fig. 4A). A negative correlation was found between the proportion of calcification and LRNC, as well as with MATX (Fig. 4B). Calcified plaques also had a larger plaque burden (Fig. 4C). LRNC associated with thinner fibrous caps, and lesions with a large proportion of MATX were associated

with smaller plaque burden and there was a negative association between calcification and IPH (Fig. 4A). In contrast, only weak correlations were seen between the degree of stenosis and plaque components.

### Association between morphology and symptomatology

Symptomatic patients had plaques with significantly higher plaque burden and LRNC compared with asymptomatic patients (Fig. 5A, B). In contrast, MATX was significantly higher in plaques from asymptomatic patients (Fig. 5C). No associations were found between either IPH or CALC and symptoms in univariable analysis (Fig. 5D, E).

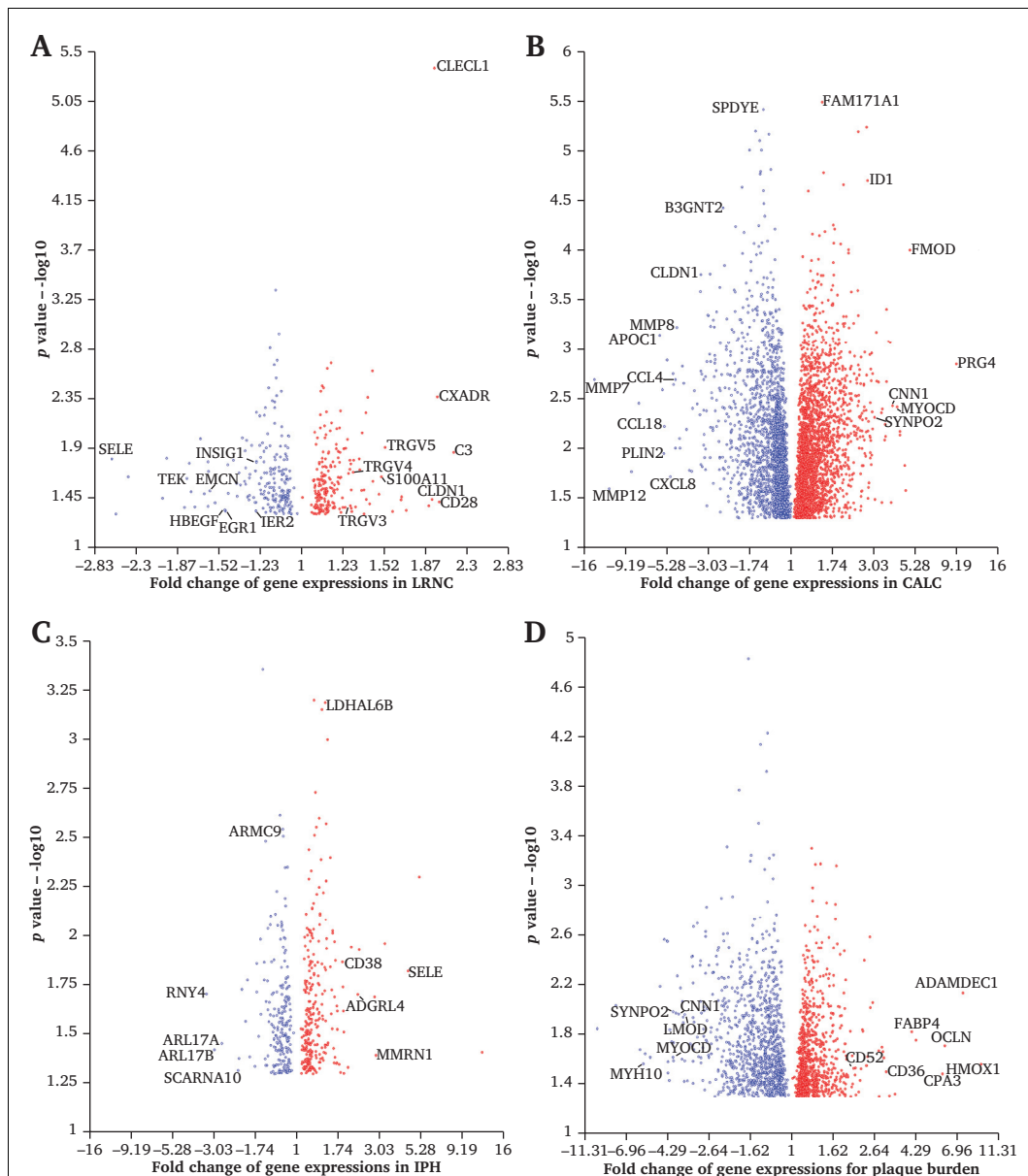


**Figure 2.** Volcano plots demonstrating differentially expressed upregulated (red) or downregulated (blue) genes in carotid plaques of selected groups from the transcriptomics cohort with high vs. low content of (A) lipid rich necrotic core (LRNC; 10 vs. 10), (B) calcification (CALC; 10 vs. 10), (C) intraplaque haemorrhage (IPH; 5 vs. 5), and (D) plaque burden volume ratio (5 vs. 5). Individual genes with high significance or fold change expression levels indicated.

The best performing multivariable predictive model, based on an averaged neural network (avNNet) developed from  $n = 63$  patients, used plaque morphology, which was superior to predictor sets built on clinical variables, the degree of stenosis (NASCET) or these in combination. Adding clinical predictors degraded, rather than improved, the performance relative to plaque morphology alone (Fig. 6A). Predictors with the greatest effect on the plaque morphology model included LRNC, MATX, and IPH (Fig. 6C). When this model was locked down and applied to plaque morphology in unseen patients ( $n = 30$ ), it performed acceptably well, as judged both by AUROC (.68) and Cohen's Kappa (.37; Fig. 6B).

## DISCUSSION

Imaging modalities to assess plaque morphology have been suggested to improve prediction of stroke risk in patients with carotid stenosis.<sup>1,2,4</sup> However, in the absence of sufficiently detailed imaging, there is a paucity of evidence coupling morphological plaque features to pathophysio-

logical processes representing plaque vulnerability. Plaque morphology, as assessed by computer based processing of conventional carotid CTA, was compared with plaque biology obtained from molecular analyses from corresponding CEA specimens. The study demonstrates strong associations between large, lipid rich and IPH containing plaques with biological processes signifying unstable lesions whereas macrocalcification was coupled to a stable molecular signature. In addition, plaque morphology was superior to the degree of stenosis in modelled symptomatology prediction. The study supports the use of plaque phenotyping by image analysis of CTAs, for improved risk stratification and management of patients with carotid atherosclerosis.

Previously, investigations with ultrasound, CTA and MRI have associated lipid rich carotid lesions with cerebral embolism,<sup>8,20,21</sup> and increased risk in lesions with a thin/fissured fibrous cap.<sup>22,23</sup> In support of these observations a significant association was observed between lipid rich plaques and symptoms, as well as fibrous cap thickness.

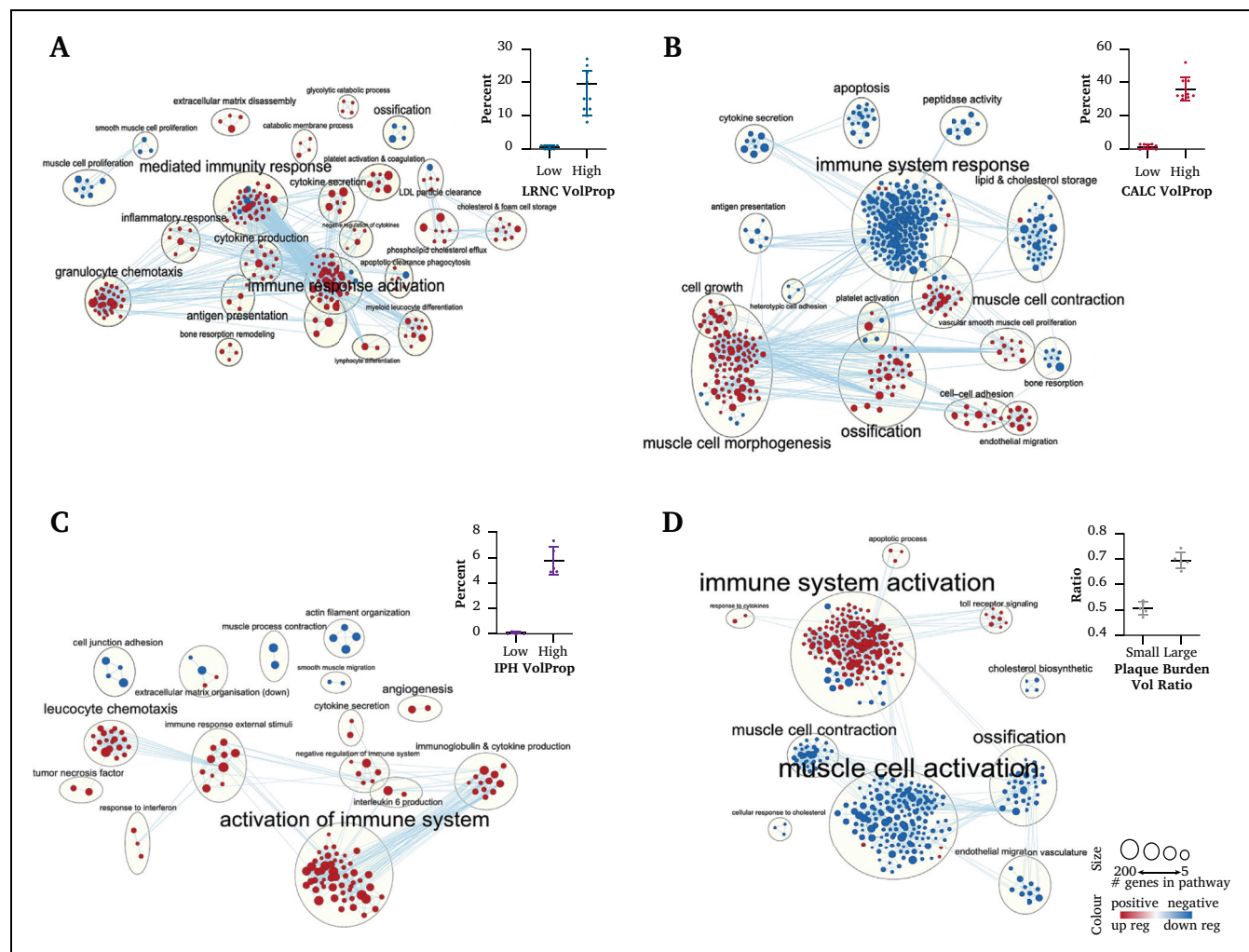
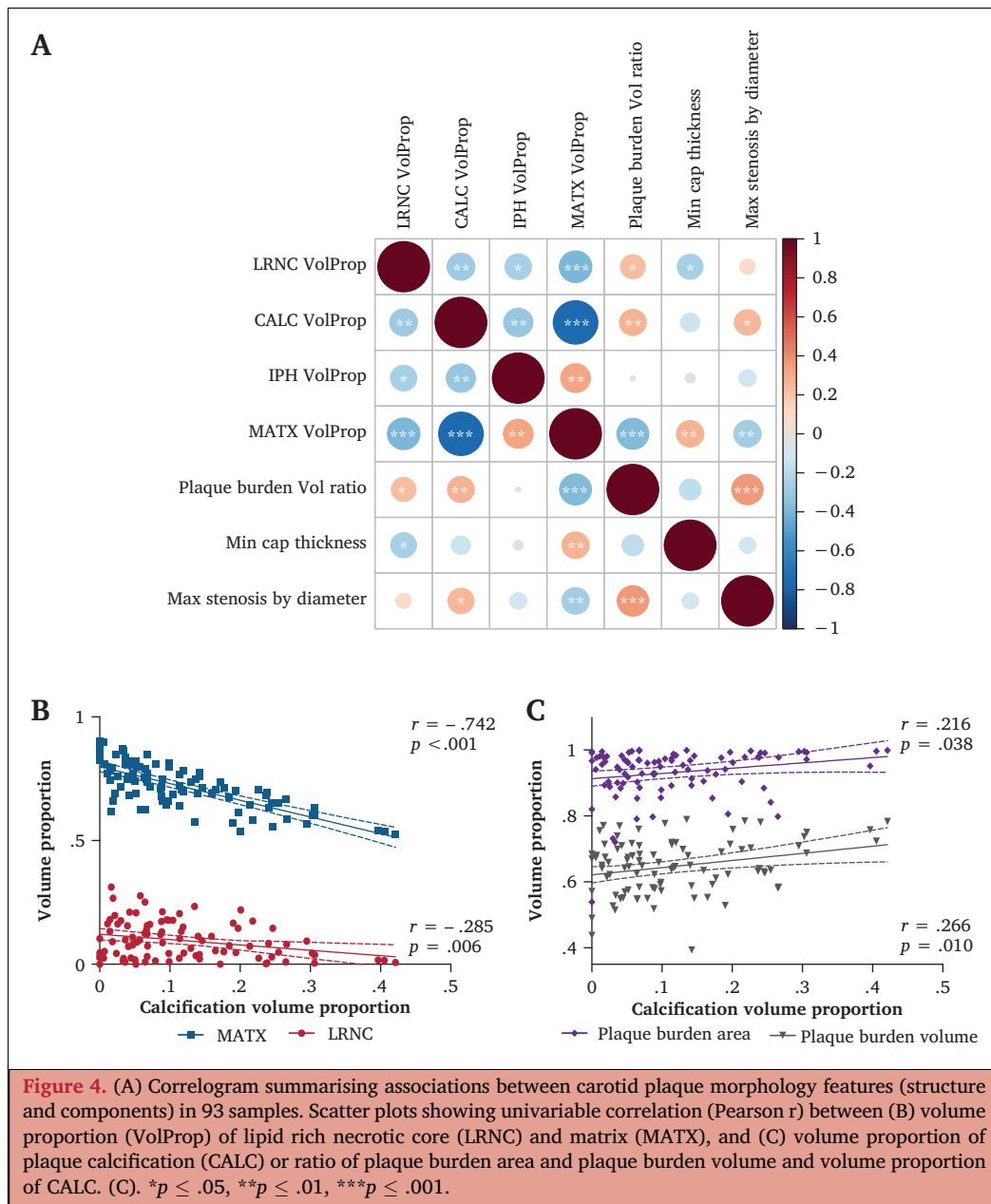


**Figure 3.** Visualisation of enriched (red) and repressed (blue) molecular pathways (i.e. biological processes) in carotid plaques of selected groups from the transcriptomics cohort with high vs. low content of (A) lipid rich necrotic core (LRNC; 10 vs. 10), (B) calcification (CALC; 10 vs. 10), (C) intraplaque haemorrhage (IPH; 5 vs. 5), and (D) plaque burden volume ratio (5 vs. 5). Inset scatter plots reflect distribution of the respective morphological feature in the analysed specimens defined high or low per volume proportion (vol prop).



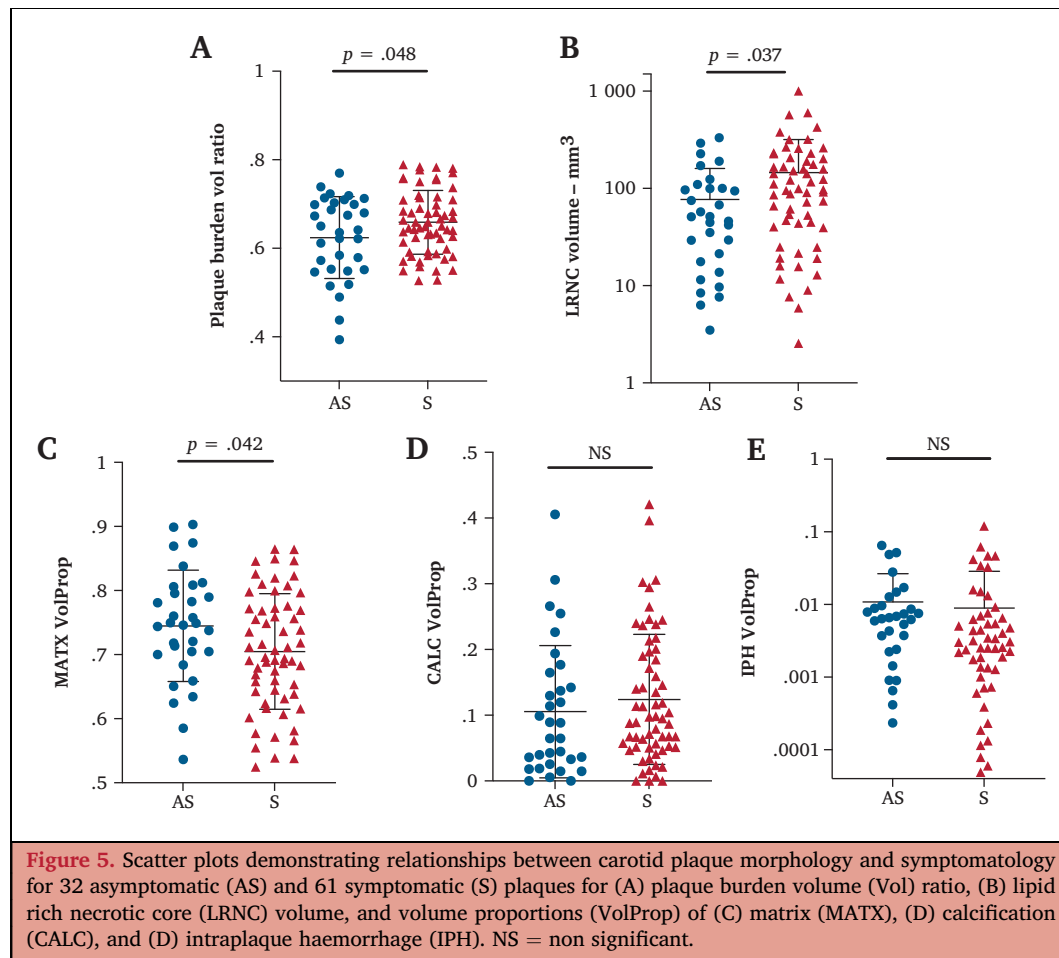
Importantly, analysis of gene expression in lesions with a large LRNC showed enrichment of processes associated with inflammation and ECM degradation and upregulation of genes previously implicated in atherosclerotic plaque inflammation.<sup>24,25</sup>

IPH is a well established feature of plaque instability,<sup>26</sup> which can be detected by MRI and is associated with increased stroke risk.<sup>27</sup> Plaques with high IPH content were shown to be dominated by inflammation and angiogenesis whereas SMC related pathways were repressed, thus supporting an association between IPH and plaque instability. It was also reported recently that carotid plaque macrocalcification signifies a more stable molecular signature.<sup>14</sup> Here, these results were validated using a different software for image analysis, with calcification representing strong enrichment of profibrotic processes whereas pathways related to inflammation and ECM degradation were

repressed. However, univariable analysis did not show any correlation between either calcification or IPH and symptoms, possibly due to the design and sample size of the study. Nevertheless, calcification was inversely associated with IPH, suggesting increased plaque stability, as previously observed in clinical studies.<sup>28</sup>

An inverse correlation was observed between the proportion of MATX and CALC. However, as plaques with low MATX overlapped with those with high calcification, this probably influenced pathway analysis and even if MATX was associated with an inflammatory signature, MATX rich plaques were rather found in asymptomatic patients. Thus, based on these results, the relevance of this plaque feature for assessment of plaque phenotype is uncertain.

Current guidelines recommend CEA for symptomatic patients with a high degree of stenosis, based on trials conducted decades ago.<sup>2</sup> Subsequently, plaque burden has



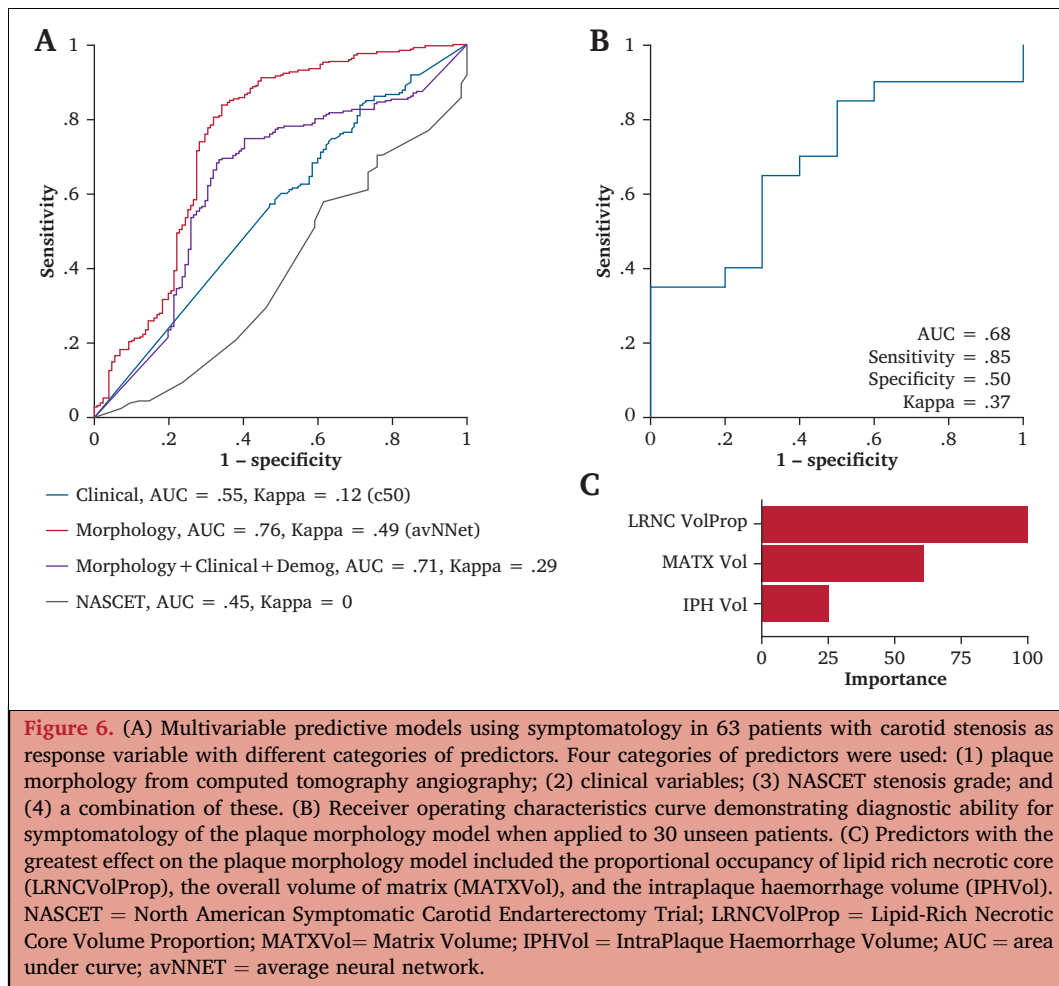
been proposed as a superior predictor of stroke risk.<sup>29,30</sup> Here, plaque burden associated with highly calcified lesions. However, whereas calcification was coupled with asymptomatic lesions, plaque burden associated with symptoms together with lipid rich plaques. In addition, the molecular profile was similar to that of lipid rich ones, but distinctly different from highly calcified lesions, suggesting that plaque burden alone is not sufficient for plaque phenotyping, which appears to require detailed analysis also of plaque components such as LRNC and calcification. In prediction modelling, plaque morphology (LRNC, MATX, IPH) was superior to the degree of stenosis in predicting symptomatology, and could also predict symptomatology in unseen patients, thus further supporting the role of plaque morphology in risk assessment of patients with carotid stenosis.<sup>1,4</sup>

Although novel, the analytical software (vascuCAP) used has been validated scientifically,<sup>8–11</sup> is approved for clinical use, and was readily implemented in this study with acceptable processing time, which is why application of this methodology in clinical practice should be encouraged.

This study is the first to demonstrate a strong association between carotid plaque morphology and biology. Nevertheless, the study has limitations, especially considering the cross sectional study design with surrogate outcomes, which should motivate prospective clinical studies for

validation. In addition, the small sample size in categories of plaque features is a limitation that probably explains the lack of significantly differentially expressed genes, where on the other hand, strong significance was obtained in pathway analyses, which is of importance since these results supported the identification of relevant biological processes. Overall, whereas the study design and cohort restricts immediate clinical translation of the results, the cohort with advanced analyses of CT images and plaques should be regarded as unique and adequate for resolving the hypothesis of the study while also providing a base on which to extend. Moreover, the transcriptomic cohort comprised patients with different degrees of plaque macrocalcification, which may not represent normal tissue heterogeneity. Finally, image analysis was performed blinded by only one observer. However, the software used includes quality assurance protocols and automated functions to mitigate subjectivity.<sup>8–11</sup>

In conclusion, this study demonstrates that image analysis of conventional CTAs for evaluation of carotid plaque morphology also reflects prevalent biological processes relevant for plaque instability. The study strengthens the concept of more sophisticated plaque phenotyping in risk stratification and management of patients with carotid stenosis and warrants further investigations in larger and prospective clinical trials.



## CONFLICT OF INTEREST

A.B. shareholder of Elucid Bioimaging.

## FUNDING

The project was funded by the Stockholm County (HMT 20180867), the Swedish Heart-Lung Foundation (20180036, 20170584, 20180244, 201602877, 20180247), the Swedish Research Council (2017-01070, 2019-02027), and Karolinska Institutet. Funding for A.B. was provided in part by the National Heart, Lung, and Blood Institute of the National Institutes of Health, USA (HL126224).

## APPENDIX A. SUPPLEMENTARY DATA

Supplementary data to this article can be found online at <https://doi.org/10.1016/j.ejvs.2021.07.011>.

## REFERENCES

- Gupta A, Marshall RS. Moving beyond luminal stenosis: imaging strategies for stroke prevention in asymptomatic carotid stenosis. *Cerebrovasc Dis* 2015;**39**:253–61.
- Aboyans V, Ricco J-B, Bartelink M-LEL, Bjorck M, Brodmann M, Cohnert T, et al. 2017 ESC Guidelines on the diagnosis and treatment of peripheral arterial diseases, in collaboration with the European Society for Vascular Surgery (ESVS). *Eur J Vasc Endovasc Surg* 2018;**55**:305–68.
- Naylor AR, Rothwell PM, Bell PRF. Overview of the principal results and secondary analyses from the European and North American randomised trials of endarterectomy for symptomatic carotid stenosis. *Eur J Vasc Endovasc Surg* 2003;**26**:115–29.
- Brinjikji W, Huston J, Rabinstein AA, Kim G-M, Lerman A, Lanzino G. Contemporary carotid imaging: from degree of stenosis to plaque vulnerability. *J Neurosurg* 2016;**124**:27–42.
- Finn AV, Nakano M, Narula J, Kolodgie FD, Virmani R. Concept of vulnerable/unstable plaque. *Arterioscler Thromb Vasc Biol* 2010;**30**:1282–92.
- ten Kate GL, Sijbrands EJ, Staub D, Coll B, ten Cate FJ, Feinstein SB, et al. Noninvasive imaging of the vulnerable atherosclerotic plaque. *Curr Probl Cardiol* 2010;**35**:556–91.
- Wintermark M, Jawadi SS, Rapp JH, Tihan T, Tong E, Glidden DV, et al. High-resolution CT imaging of carotid artery atherosclerotic plaques. *AJNR Am J Neuroradiol* 2008;**29**:875–82.
- Zhu G, Li Y, Ding V, Jiang B, Ball RL, Rodriguez F, et al. Semi-automated characterization of carotid artery plaque features from computed tomography angiography to predict atherosclerotic cardiovascular disease risk score. *J Comput Assist Tomogr* 2019;**43**:452–9.
- Abdelrahman KM, Chen MY, Dey AK, Virmani R, Finn AV, Khamis RY, et al. Coronary computed tomography angiography from clinical uses to emerging technologies: JACC State-of-the-Art Review. *J Am Coll Cardiol* 2020;**76**:1226–43.
- Chrencik MT, Khan AA, Luther L, Anthony L, Yokemick J, Patel J, et al. Quantitative assessment of carotid plaque morphology (geometry and tissue composition) using computed tomography angiography. *J Vasc Surg* 2019;**70**:858–68.

- 11 Sheahan M, Ma X, Paik D, Obuchowski NA, St.Pierre S, Newman WP, et al. Atherosclerotic plaque tissue: noninvasive quantitative assessment of characteristics with software-aided measurements from conventional CT angiography. *Radiology* 2017;**286**:622–31.
- 12 van Assen M, Varga-Szemes A, Schoepf UJ, Duguay TM, Hudson HT, Egorova S, et al. Automated plaque analysis for the prognostication of major adverse cardiac events. *Eur J Radiol* 2019;**116**:76–83.
- 13 Choi H, Uceda DE, Dey AK, Abdelrahman KM, Aksentijevich M, Rodante JA, et al. Treatment of psoriasis with biologic therapy is associated with improvement of coronary artery plaque lipid-rich necrotic core: results from a prospective, observational Study. *Circ Cardiovasc Imaging* 2020;**13**:e011199.
- 14 Karlöf E, Seime T, Dias N, Lengquist M, Witasp A, Almqvist H, et al. Correlation of computed tomography with carotid plaque transcriptomes associates calcification with lesion-stabilization. *Atherosclerosis* 2019;**288**:175–85.
- 15 Perisic L, Aldi S, Sun Y, Folkersen L, Razuvaev A, Roy J, et al. Gene expression signatures, pathways and networks in carotid atherosclerosis. *J Intern Med* 2016;**279**:293–308.
- 16 Ritchie ME, Phipson B, Wu D, Hu Y, Law CW, Shi W, et al. limma powers differential expression analyses for RNA-sequencing and microarray studies. *Nucleic Acids Res* 2015;**43**:e47.
- 17 Subramanian A, Tamayo P, Mootha VK, Mukherjee S, Ebert BL, Gillette MA, et al. Gene set enrichment analysis: a knowledge-based approach for interpreting genome-wide expression profiles. *Proc Natl Acad Sci U S A* 2005;**102**:15545–50.
- 18 Reimand J, Isserlin R, Voisin V, Kucera M, Tannus-Lopes C, Rostamianfar A, et al. Pathway enrichment analysis and visualization of omics data using g:Profiler, GSEA, Cytoscape and EnrichmentMap. *Nat Protoc* 2019;**14**:482–517.
- 19 Kuhn M, Johnson K. *Applied predictive modeling*. New York: Springer; 2013.
- 20 Nicolaidis AN, Kakkos SK, Kyriacou E, Griffin M, Sabetai M, Thomas DJ, et al. Asymptomatic internal carotid artery stenosis and cerebrovascular risk stratification. *J Vasc Surg* 2010;**52**:1486–96.
- 21 Gupta A, Baradaran H, Schweitzer AD, Kamel H, Pandya A, Delgado D, et al. Carotid plaque MRI and stroke risk: a systematic review and meta-analysis. *Stroke* 2013;**44**:3071–7.
- 22 Kakkos SK, Griffin MB, Nicolaidis AN, Kyriacou E, Sabetai MM, Tegos T, et al. The size of juxtaluminar hypoechoic area in ultrasound images of asymptomatic carotid plaques predicts the occurrence of stroke. *J Vasc Surg* 2013;**57**:609–18.
- 23 Sun J, Zhao X-Q, Balu N, Neradilek MB, Isquith DA, Yamada K, et al. Carotid plaque lipid content and fibrous cap status predict systemic CV outcomes: the MRI substudy in AIM-HIGH. *JACC Cardiovasc Imaging* 2017;**10**:241–9.
- 24 Hertle E, van Greevenbroek MM, Arts IC, van der Kallen CJ, Geijselaers SL, Feskens EJ, et al. Distinct associations of complement C3a and its precursor C3 with atherosclerosis and cardiovascular disease. The CODAM study. *Thromb Haemost* 2014;**111**:1102–11.
- 25 Nilchian A, Plant E, Parniewska MM, Santiago A, Rossignoli A, Skogsberg J, et al. Induction of the coxsackievirus and adenovirus receptor in macrophages during the formation of atherosclerotic plaques. *J Infect Dis* 2020;**222**:2041–51.
- 26 Michel J-B, Martin-Ventura JL, Nicoletti A, Ho-Tin-Noé B. Pathology of human plaque vulnerability: mechanisms and consequences of intraplaque haemorrhages. *Atherosclerosis* 2014;**234**:311–9.
- 27 Porcu M, Anzidei M, Suri JS, Wasserman B A, Anzalone N, Lucatelli P, et al. Carotid artery imaging: the study of intra-plaque vascularization and hemorrhage in the era of the "vulnerable" plaque. *J Neuroradiol* 2020;**47**:464–72.
- 28 Kwee RM. Systematic review on the association between calcification in carotid plaques and clinical ischemic symptoms. *J Vasc Surg* 2010;**51**:1015–25.
- 29 Rozie S, de Weert TT, de Mony C, Homburg PJ, Tanghe HLJ, Dippel DWJ, et al. Atherosclerotic plaque volume and composition in symptomatic carotid arteries assessed with multidetector CT angiography; relationship with severity of stenosis and cardiovascular risk factors. *Eur Radiol* 2009;**19**:2294–301.
- 30 Murgia A, Balestrieri A, Francone M, Lucatelli P, Scapin E, Buckler A, Micheletti G, Faa G, Conti M, Suri JS, Guglielmi G, Carriero A, Saba L. Plaque imaging volume analysis: technique and application. *Cardiovasc Diagn Ther* 2020;**10**:1032–47.